Lyophilization of Pharmaceutical Injections: Theoretical Physical Model

N. F. H. HO * and T. J. ROSEMAN ‡x

Received December 28, 1978, from the *College of Pharmacy, University of Michigan, Ann Arbor, MI 48109, and ‡Pharmacy Research, The Upjohn Company, Kalamazoo, MI 49001. Accepted for publication March 28, 1979.

Abstract □ A physical model for the lyophilization kinetics of parenteral formulations is presented. Mathematical relationships are derived, which involve the simultaneous change in the receding boundary of the ice–vapor interface with time as well as water vapor diffusion across the dry porous matrix and boundary layer. Heat from an external heat source is transferred across the frozen solution to the receding ice surface. The model predicts that the water lost and the receding boundary distance are linearly related to the square root of time when lyophilization is matrix controlled. The mathematical descriptions are predictive of the physicochemical and transport events and can lead to the design of quantitative experiments to relate theory to formulation design.

Keyphrases □ Lyophilization—physicochemical model, parenteral formulations □ Models, physicochemical—lyophilization, parenteral formulations □ Dosage forms, parenteral—lyophilization, physicochemical model

Lyophilization, commonly called freeze drying, involves the removal of water from a frozen substance by sublimation and mass transfer under vacuum conditions and at temperatures less than the eutectic temperature of the multicomponent aqueous solution. Its importance and usage as a drying process are well known in the pharmaceutical and food industries and in biological laboratories (1–4). The lyophilization of parenteral products is not problem free. Rejection rates are attributed to melt-backs or nonuniformity in the color of the dried drug matrix, which is not necessarily accompanied by decreased potency. The total drying cycles are often long, ranging from 24 to 48 hr, and approaches toward optimizing the drying cycle and time of complete drying are generally empirical.

Much interest in theoretical kinetic models and their application to the freeze drying of foods and model systems is found in the literature (2, 5–8). These models have addressed both the mass transfer process and the heat transfer problem, including the physical factors governing the kinetics.

DeLuca and Lachman (9), in reporting on the freeze drying of pharmaceutical products, emphasized the theory and method of determining eutectic temperatures of drug formulations and also the influence of the eutectic temperature on practical lyophilization cycles. They investigated the effect of various metal trays on heat transfer during lyophilization (10). Effects of additives in preformulation systems on melting behavior and eutectic temperatures have been investigated (11). The macroscopic appearance of frozen solutions and dried samples has been studied (12).

This paper describes a physical model for lyophilization. The model is based on the principles of physical chemistry and on the laws of transport with accompanying mathematics and is described in a manner amenable to well-designed experimental approaches, mechanistic interpretation, quantitation of physically relevant parameters, and predictiveness. The lyophilization of parenteral products is one area of pharmaceutical processing that presents nearly an ideal situation for relating theory and practice. With a basic understanding about lyophilization and the rate-determining physicochemical conditions, a rational approach to optimizing the formulation and process conditions can evolve.

THEORY

Physical Model—The physical model describing lyophilization of a frozen aqueous solution containing drug and a matrix-building substance (*e.g.*, mannitol or lactose) should be analogous to the well-known model for drug release from an inert and insoluble matrix (13, 14). As shown in Fig. 1, it involves the simultaneous change in the receding boundary with time, phase transition at the ice–vapor interface, and water vapor diffusion across both the pore path length of the matrix and the diffusional boundary layer just outside the matrix. No unusual water vapor accumulation is assumed here, *i.e.*, sink conditions.

It is taken that the matrix pores are continuous and fairly uniform, with no significant presence of end pores and isolated ice pockets; hence, the receding boundary is sharp. The freezing rates have marked influence on the distribution, quality, and sizes of the pores and, consequently, on the overall lyophilization kinetics (15, 16). In the general situation, water vapor transport occurs by ordinary (viscous) and free molecular flow according to well-established laws of kinetic motion of gases in pores. The general case also includes water vapor adsorption on polar surfaces with surface diffusion.

Throughout the following sections, the definitions of various terms with their corresponding units are presented so that the paired set of units will yield the correct calculations.

Flux Expressions—The mass transport of water vapor across the boundary layer at the matrix surface is expressed by:

$$J = \frac{DC_0}{H} = (\mathrm{PC})(C_0) \qquad \text{(Eq. 1)}$$

where:

J = flux per unit of cross-sectional area
D = diffusion coefficient of the water vapor, square centimeters per second
H = boundary layer thickness
PC = permeability coefficient of the boundary layer, centimeters per second
C_0 = concentration of vapor at the matrix surface at $x = 0$

The flux per unit of cross-sectional area across the matrix pores for the viscous, molecular, and surface diffusion mechanism is:

$$J_M = \frac{\epsilon}{\tau} D_p \frac{dC}{dx} + \frac{\epsilon}{\tau} D^* \frac{dC^*}{dx} \qquad \text{(Eq. 2)}$$

where:

J_M = flux per unit of area
D_p = effective diffusion coefficient for viscous and molecular flow
D^* = surface diffusion coefficient
ϵ = volume fraction of water in the total system
τ = tortuosity factor ≥ 1.0 and usually 3.0
C = concentration of vapor in the pores
C^* = concentration of vapor molecules adsorbed on the matrix surface in the pores

According to the Langmuir adsorption isotherm:

$$C^* = \frac{k_1 k_2 C}{1 + k_1 C} \qquad \text{(Eq. 3)}$$

0022-3549/79/0900-1170$01.00/0
© 1979, American Pharmaceutical Association

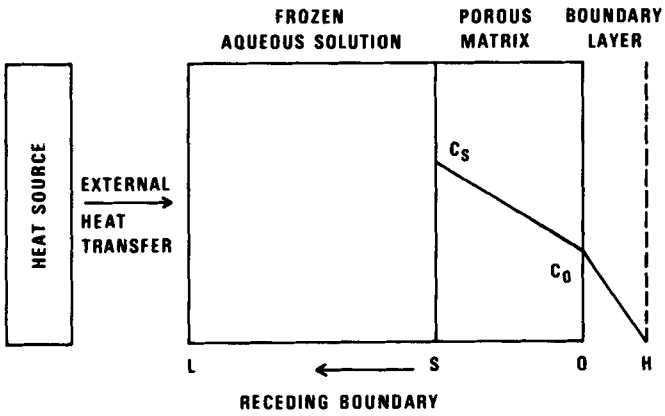

Figure 1—*Physical model for lyophilization involving simultaneous receding boundary of ice-vapor interface and water vapor diffusion across porous matrix and boundary layer and into sink with time. Heat from an external heat source is transferred across frozen solution to receding ice surface.*

where k_1 is the adsorption coefficient and k_2 is the maximum surface concentration of adsorption sites.

Utilizing the chain rule, one gets:

$$\frac{dC^*}{dx} = \left(\frac{dC^*}{dC}\right)\left(\frac{dC}{dx}\right) \quad \text{(Eq. 4)}$$

whereupon:

$$\frac{dC^*}{dx} = \frac{k_1 k_2}{(1 + k_1 C)^2}\left(\frac{dC}{dx}\right) \quad \text{(Eq. 5)}$$

With the condition of $k_1 C \ll 1$, Eq. 5 is simplified considerably to:

$$\frac{dC^*}{dx} = k\frac{dC}{dx} \quad \text{(Eq. 6)}$$

where $k = k_1 k_2$. This assumption in the Henry's law region of the adsorption isotherm is reasonable because of the low vapor pressure conditions employed in lyophilization. It follows that:

$$J_M = \left(\frac{\epsilon}{\tau}\right)(D_p + kD^*)\left(\frac{dC}{dx}\right) \quad \text{(Eq. 7)}$$

and, allowing for linear concentration gradients:

$$J_M = \frac{(D_e)(C_s - C_0)}{S} \quad \text{(Eq. 8)}$$

where:

$$D_e = \left(\frac{\epsilon}{\tau}\right)(D_p + kD^*) \quad \text{(Eq. 9)}$$

and S is the receding boundary distance and C_s is the concentration of water vapor at the ice surface.

The continuity of mass flow at $x = 0$ is given by:

$$J = J_M \quad \text{(Eq. 10)}$$

Accordingly, one readily gets:

$$J_M = \frac{C_s}{\frac{S}{D_e} + \frac{1}{PC}} \quad \text{(Eq. 11)}$$

and, in turn:

$$J_M = \frac{dQ}{dt} \quad \text{(Eq. 12)}$$

where Q is the amount of water released from the system per unit area and t is time.

Change in Receding Boundary in Matrix and Amount of Water Released with Time—By using a linear approximation, it can be seen in Fig. 1 that:

$$Q = S(A - n\epsilon C_s) \quad \text{(Eq. 13)}$$

where A is the amount of water per unit volume of the system and n is a constant whereby $0.5 \leq n < 1.0$. If sink conditions exist at $x = 0$, *i.e.*, there is no appreciable water vapor accumulation at the matrix surface, $n = 0.5$; otherwise, $n > 0.5$. As will be seen in the next section, A will be much greater than $n\epsilon C_s$ such that:

$$Q = AS \quad \text{(Eq. 14)}$$

Thus:

$$\frac{dQ}{dt} = A\frac{dS}{dt} \quad \text{(Eq. 15)}$$

By combining Eqs. 11, 12, and 15 and integrating between the limits of $S(0) = 0$ and $S(t)$, the change in the receding boundary with time is:

$$S^2 + \frac{2D_e S}{PC} = \frac{2D_e C_s t}{A} \quad \text{(Eq. 16)}$$

$$S = -\frac{D_e}{PC} + \sqrt{\left(\frac{D_e}{PC}\right)^2 + \frac{2D_e C_s t}{A}} \quad \text{(Eq. 17)}$$

With Eqs. 11 and 14, the change in the amount of water released per unit of cross-sectional area is given by the quadratic expression:

$$Q^2 + \frac{2AD_e Q}{PC} = 2AD_e C_s t \quad \text{(Eq. 18)}$$

$$Q = A\left[-\frac{D_e}{PC} + \sqrt{\left(\frac{D_e}{PC}\right)^2 + \frac{2D_e C_s t}{A}}\right] \quad \text{(Eq. 19)}$$

It is readily observed in Eqs. 17 and 18 that when the transport rate is controlled by the matrix, the kinetics directly follow the square root of time relationship. Thus:

$$S = \sqrt{\frac{2D_e C_s t}{A}} \quad \text{(Eq. 20)}$$

$$\frac{dS}{dt} = \sqrt{\frac{D_e C_s}{2At}} \quad \text{(Eq. 21)}$$

$$Q = \sqrt{2D_e AC_s t} \quad \text{(Eq. 22)}$$

$$\frac{dQ}{dt} = \sqrt{\frac{D_e AC_s}{2t}} \quad \text{(Eq. 23)}$$

It is explicit in the development of the theory that C_s is constant throughout time; in other words, the vapor pressure and temperature at the ice surface are constant.

Surface Concentration of Water Vapor and Pressure—The water vapor concentration at the ice surface, C_s in grams per cubic centimeter, may be approximated by the ideal gas law:

$$C_s = \frac{P_s M}{1000RT_s} \quad \text{(Eq. 24)}$$

where:

P_s = vapor pressure of ice, atmospheres
R = gas constant, 0.08205 liter atm $°K^{-1}$ $mole^{-1}$
T_s = absolute temperature at the ice surface
M = molecular weight of water

The vapor pressure on ice, P_{mm} in millimeters of mercury, is given by the following relationship (18) or in critical tables:

$$\log P_{mm} = -\frac{2445.5656}{T} + 8.2312 \log T - 1677.006 \times 10^{-5} T + 120514 \times 10^{-10} T^2 - 6.757169 \quad \text{(Eq. 25)}$$

It can be determined that at −20°, P_s is 1.02×10^{-3} atm and C_s is 8.88×10^{-7} g/cm^3; at −10°, P_s and C_s are 2.56×10^{-3} atm and 2.14×10^{-6} g/cm^3, respectively. Accordingly, the cited condition of $A \gg n\epsilon C_s$ is justified since the amount of water per cubic centimeter, A, is generally ≥ 0.5 g/cm^3.

Diffusivity of Water Vapor in Porous Matrix—According to the kinetic theory of gases, the flow of vapor molecules in fine pores depends on the mean free path relative to the pore radius (18, 19). The Knudsen number, Kn, is defined by:

$$Kn = \frac{\lambda}{r_e} \quad \text{(Eq. 26)}$$

where λ is mean free path in centimeters and r_e is the effective pore radius in centimeters. The mean free path, the distance a molecule travels before

Table I—Estimates of the Water Vapor Diffusion Coefficients at Low Temperatures and Vapor Pressures for Different Effective Pore Sizes [a]

T_s	P_s, mm Hg	r_e, μm	Diffusion Coefficient × 10^{-2} cm²/sec			Knudsen Number
			D_v	D_K	D_{pore}	
−20°	0.779	25	2.68	0.91	0.68	10.2
		50	2.68	1.82	1.08	5.1
		100	2.68	3.64	1.54	2.5
		200	2.68	7.28	1.96	1.27
−30°	0.293	25	6.78	0.89	0.79	27.6
		50	6.78	1.78	1.41	13.8
		100	6.78	3.57	2.34	6.9
		200	6.78	7.14	3.48	3.5

[a] Values used were: M = 18, P_{out} = 10^{-3} mm, σ_{H_2O} = 2.641, Ω_D = 2.613 at −20° and 2.662 at −30°, and λ = 254 μm at − 20° and 690 μm at −30°.

colliding with another one, is further given by:

$$\lambda = \frac{1}{\sqrt{2}(\pi d^2 N)} \qquad \text{(Eq. 27)}$$

where d is the molecular diameter of water vapor (3.46 Å) and N is the number of molecules per cubic centimeter. In turn:

$$N = \frac{PN_{Av}}{1000RT} \qquad \text{(Eq. 28)}$$

where N_{Av} is Avogadro's number, P is pressure, and the other terms are as defined previously. As can be seen, λ is inversely proportional to the vapor concentration or pressure.

Gas flow in pores is generally divided into four regimes (20): (*a*) $Kn < 0.01$, viscous flow; (*b*) $0.01 < Kn < 0.1$, viscous slip flow; (*c*) $0.1 < Kn < 3.0$, transition; and (*d*) $3.0 < Kn$, free molecular flow. As the vapor pressure approaches near-vacuum conditions, the character of the vapor flow progressively changes from viscous to free molecular flow. In viscous flow, the diffusional resistance arises from intermolecular collisions; at the other extreme, the diffusional resistance in free molecular flow is due to the collision of gas molecules with the pore surface. At pressures below the viscous limit previously indicated, the viscous flow must be corrected for slip flow about the pore walls.

At this point, it is useful to determine the flow regime under which lyophilization (low pressures and low temperatures below the eutectic temperature) generally occurs. For example, when the average pressure in the pores is equal to one-half the vapor pressure of ice at −20°, λ is 1.27 × 10^{-2} cm or 127 μm by Eqs. 25, 27, and 28; at −30°, λ is 345 μm. Since the effective pore radius is expected to be <1000 μm, Kn will be >0.1. Accordingly, the pore transport of vapor will occur most likely within the transition of viscous to free molecular flow regimes.

In the Knudsen region of free molecular flow, the water vapor diffusion coefficient (19, 21) is:

$$D_K = \left(\frac{2r_e}{3}\right)\left(\frac{8RT}{\pi M}\right)^{1/2} \qquad \text{(Eq. 29)}$$

When the following parameters are defined with the units indicated, *i.e.*, r_e is the effective pore radius in centimeters, R is the gas constant taken as 8.315 × 10^7 ergs deg^{-1} mole^{-1}, M is the molecular weight, and T is the average absolute temperature in the pores, then D_K will have units of square centimeters per second. Here, λ is much larger than r_e so that the collision of gas molecules with the walls is more probable than that between molecules.

In viscous flow, the ordinary diffusion coefficient for gases, allowing for mutual interaction, may be employed (22):

$$D_v = \frac{0.002627T^{3/2}}{\sigma^2_{H_2O}\Omega_D P_{ave} M^{1/2}} \qquad \text{(Eq. 30)}$$

where:

D_v = diffusion coefficient for viscous flow, square centimeters per second

P_{ave} = average pressure in the pores in atmospheres with respect to the vapor pressure of ice and the pressure outside the porous matrix
$= (P_s - P_0)/2$

σ_{H_2O} = Lennard–Jones force constant for water

Ω_D = temperature-dependent collision integral

The σ_{H_2O} (= 2.641 Å) and Ω_D constants are found in various sources (22–24). The values of Ω_D are 2.613 at −20° and 2.662 at −30°. As can be seen, D_v can be rather large at low pressures.

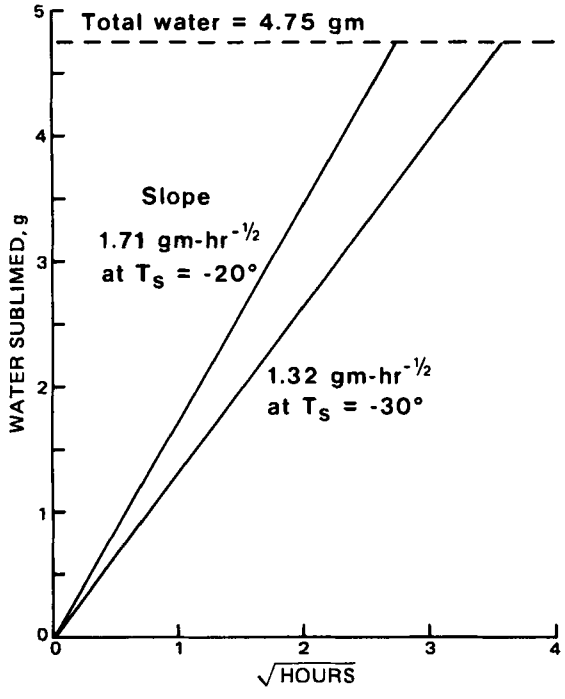

Figure 2—*Changes in amount of water lyophilized with time for two surface temperatures at the receding front. Theoretical plots are based on parameter values in Table II.*

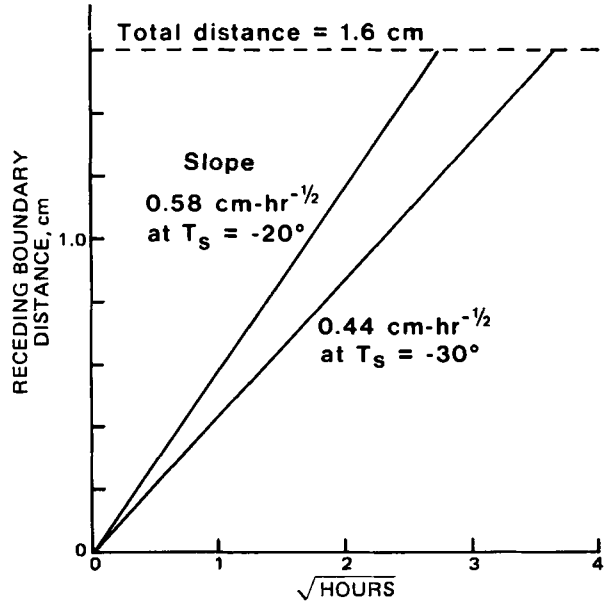

Figure 3—*Receding boundary distance changes with time for two surface temperatures at the receding front. Theoretical plots are based on parameter values in Table II.*

Table II—Physical Parameters Used in Theoretical Computations of Lyophilization Rates[a]

T_s	P_s, mm Hg	r_e, μm	D_v, cm²/sec	D_κ, cm²/sec	A, g/ml	ϵ	τ
−20°	0.779	100	2.68×10^2	3.64×10^2	0.95	0.95	3.0
−30°	0.293	100	6.78×10^2	3.57×10^2	0.95	0.95	3.0

[a] A 5-ml sample was in a 2.0-cm i.d. vial. Total amount of water was 4.75 g.

The transition of viscous to Knudsen's free molecular flow is not precise. While the former is pressure dependent, the latter is not. For practical purposes, Pollard and Present (25) provided an approximate expression:

$$D_P = \frac{1}{1/D_v + 1/D_K} \qquad \text{(Eq. 31)}$$

Although the mathematical form implies a physical situation (which is not real here) whereby the pore resistance due to viscous flow is in series with the pore resistance due to free molecular flow, the expression does allow an adequately smooth transition for computational purposes. When $D_v \gg D_K$, Knudsen diffusion will be the rate-controlling mechanism.

Table I gives estimates of the diffusion coefficients of water vapor at low temperatures and pressures for different pore radii. At −20° where the vapor pressure of ice is 0.779 mm Hg and the outside pressure is 10^{-3} mm Hg, the D_{pore} is 0.68–1.96 × 10^2 cm²/sec for average pore radii of 25–200 μm. When the average pore radius (r_e) is 25 μm, the vapor transport is ~ 75% controlled by Knudsen diffusion; when r_e = 200 μm, the transport is largely controlled by viscous flow. At the low surface temperature condition of −30°, Knudsen flow kinetics prevail.

Owing to the presence of the many hydroxyl groups in lactose and mannitol, usually employed as matrix builders, water adsorption is likely, *e.g.*, the water vapor adsorption on standard cellulose and cotton cellulose (26), for the latter of which the heat of adsorption is 15.7 kcal/mole. At low vapor densities, the mobility of adsorbed molecules occurs mechanistically by two-dimensional "random walk" (27):

$$D^* = \frac{\lambda_s^2}{4\tau^*} \qquad \text{(Eq. 32)}$$

where D^* is the surface diffusion coefficient in square centimeters per second, λ_s is the distance between adsorption sites (3 × 10^{-8} cm), and τ^* is the average residence time between lateral jumps in seconds.

With:

$$\tau^* = \tau_0^{\cdot} e^{E^*/RT} \qquad \text{(Eq. 33)}$$

where:

$\tau_0^{\cdot}$ = residence time related to the vibrational frequency of the solid surface atoms
$\nu^* = 1/\tau_0^{\cdot}$, the jump frequency being ~10^{12} sec^{-1}
E^* = activation energy for surface diffusion
RT = thermal energy

Eq. 32 becomes:

$$D^* = \frac{\lambda_s^2 \nu^*}{4} e^{-E^*/RT} \qquad \text{(Eq. 34)}$$

It is assumed that the surface is isotropic and that the vapor pressure is low. At higher pressures, viscous surface diffusion becomes increasingly important due to collision with adsorbed molecules. Gilliland *et al.* (28) let E^* vary linearly with the differential heat of adsorption, with the result that more strongly adsorbed molecules are less mobile. For physically adsorbed molecules, D^* values are 10^{-2}–10^{-5} cm²/sec; for chemically adsorbed species, they range from 10^{-5} to 10^{-13} cm²/sec (29).

Final Expressions of Matrix-Controlled Lyophilization Kinetics—When the diffusional rate is controlled by the matrix, it is expected to follow the square root of time law. Replacing C_s in Eqs. 20 and 22 with 24 and expanding D_e, one gets for the receding boundary:

$$S = \left[\frac{\epsilon}{\tau}\left(\frac{1}{1/D_v + 1/D_K} + kD^*\right)\left(\frac{MP_s}{500ART_s}\right)(t)\right]^{1/2} \qquad \text{(Eq. 35)}$$

Likewise, the amount of water released per unit of cross-sectional area is:

$$Q = \left[\frac{\epsilon}{\tau}\left(\frac{1}{1/D_v + 1/D_K} + kD^*\right)\left(\frac{AMP_s}{500RT_s}\right)(t)\right]^{1/2} \qquad \text{(Eq. 36)}$$

Interrelation of Heat and Mass Transfer—The steady-state rate of heat transfer from an external heat source and across the frozen region to supply the necessary sublimation energy at the ice front (Fig. 1) is:

$$\frac{dU}{dt} = (h_{ex})(T_{ex} - T_L) = \left(\frac{\kappa}{L - S}\right)(T_L - T_s) \qquad \text{(Eq. 37)}$$

or:

$$\frac{dU}{dt} = \frac{(T_{ex} - T_s)}{\frac{1}{h_{ex}} + \frac{L}{\kappa} - \frac{S}{\kappa}} \qquad \text{(Eq. 38)}$$

and, in turn, it is related to the lyophilization rate by:

$$\left.\frac{dU}{dt}\right|_{x=-S} = \Delta H_{sub}\frac{dQ}{dt} \qquad \text{(Eq. 39)}$$

where:

dU/dt = heat flux per unit of area, calories per second per square centimeter
h_{ex} = external heat transfer coefficient, calories per second per square centimeter per degree
κ = thermal conductivity, calories per second per centimeter per degree
S = receding boundary, centimeters
T_{ex} = temperature of the external heat source
T_L = temperature at $x = -L$ of the frozen region
T_s = temperature of the ice–vapor interface
ΔH_{sub} = heat of sublimation, 600–700 cal/g
dQ/dt = lyophilization rate per square centimeter

It can be seen in Eq. 38 that when $\kappa/L \gg h_{ex}$, the supply of heat to the receding ice front will be controlled by the external heat transfer system (geometry, method of heating, heat transfer mechanism, *etc.*).

Combining Eqs. 11, 38, and 39 and assuming that T_s does not change with time[1], one obtains:

$$S = -\beta\kappa + \sqrt{(\beta\kappa)^2 + \frac{(2\kappa)(T_{ex} - T_s)(t)}{A\,\Delta H_{sub}}} \qquad \text{(Eq. 40)}$$

$$Q = -A\beta\kappa + \sqrt{(A\beta\kappa)^2 + \frac{(2A\kappa)(T_{ex} - T_s)(t)}{\Delta H_{sub}}} \qquad \text{(Eq. 41)}$$

with:

$$\beta = \frac{1}{h_{ex}} + \frac{L}{\kappa} \qquad \text{(Eq. 42)}$$

From the linear portion of a Q or S *versus* $\sqrt{t}$ plot, one can estimate the thermal conductivity, κ, of the frozen system once T_{ex} and T_s are known.

In the region where Eq. 41 is applicable, the lyophilization rates are affected not only by external heat transfer factors due to the equipment but also by internal thermal factors characteristic of the material being dried. In contrast, the derived rates as described previously (*e.g.*, Eqs. 35 and 36) focus attention on the frozen system formulation, the ice–vapor interface, and the mass transfer processes within the growing dry matrix.

DISCUSSION

To demonstrate the predictions of the model, the lyophilization of a 5% solution in which 5 ml is frozen in a 2-cm diameter cylinder is used as an example. Let the solid additives (drug and matrix builder) and water have a density of unity. Therefore, the amount of water per unit volume is 0.95 and the porosity, approximated by the volume fraction of water, is also 0.95. The total amount of water is 4.75 g. The tortuosity and the pore radius are taken to be 3.0 and 100 μm, respectively. Wall effects are assumed to be negligible. Two surface temperature cases are considered: −20 and −30°.

[1] When the temperature at the ice–vapor interface changes with the receding boundary, it can be evaluated from Eq. 37; thus:

$$T_s = T_L - \left(\frac{h_{ex}}{\kappa}\right)(T_{ex} - T_L)(L - S)$$

Here, T_s increases with the receding boundary thickness until $S = L$, whereby $T_s = T_L$. If $h_{ex}/\kappa \ll 1.0$, then $T_s \simeq T_L$.

The physical parameters for these conditions are summarized in Table II. Figure 2 shows the amount of water lyophilized *versus* square root of time curves generated by the steady-state expression described in Eq. 36, whereby the surface diffusion consideration is neglected. As can be seen, the lyophilization rates are faster at −20° than at −30°. Lyophilization is completed in 7.7 hr at the surface temperature of −20° and in 13 hr at −30°. The linear profiles of the receding boundary with the square root of time according to Eq. 35 are observed in Fig. 3.

Future studies will be directed toward the experimental verification of the interdependence of the variables described in this paper.

REFERENCES

(1) E. Flosdorf, "Freeze Drying," Reinhold, New York, N.Y., 1949.

(2) C. J. King, "Freeze Drying of Foods," CRC Press, Cleveland, Ohio, 1971.

(3) R. Noyes, "Freeze Drying of Foods and Biologicals," Noyes Development Corp., Park Ridge, N.J., 1968.

(4) S. A. Goldblith, L. Rey, and W. W. Rothmayr, "Freeze Drying and Advanced Food Technology," Academic, New York, N.Y., 1975.

(5) L. Rey, "Advances in Freeze Drying," Hermann, Paris, France, 1966, pp. 39, 55, 75.

(6) J. L. Stephenson, *Bull. Math. Biophys.*, **15**, 411 (1953).

(7) D. F. Dyer and J. E. Sunderland, *J. Heat Trans.*, **90**, 379 (1968).

(8) *Ibid.*, **93**, 427 (1971).

(9) P. DeLuca and L. Lachman, *J. Pharm. Sci.*, **54**, 617, 1411 (1965).

(10) P. DeLuca and L. Lachman, *Bull. Parenter. Drug Assoc.*, **20**, 65 (1966).

(11) R. M. Patel and A. Hurwitz, *J. Pharm. Sci.*, **61**, 1806 (1972).

(12) K. Ito, *Chem. Pharm. Bull.*, **18**, 1509, 1519 (1970).

(13) T. Higuchi, *J. Pharm. Sci.*, **52**, 1145 (1963).

(14) S. J. Desai, P. Singh, A. P. Simonelli, and W. I. Higuchi, *ibid.*, **55**, 1224, 1230 (1966).

(15) A. P. MacKenzie, *Bull. Parenter. Drug Assoc.*, **20**, 101 (1966).

(16) D. G. Quast and M. Karel, *J. Food Sci.*, **33**, 170 (1968).

(17) N. E. Dorsey, "Properties of Ordinary Water Substance," Reinhold, New York, N.Y., 1940, p. 598.

(18) E. H. Kennard, "Kinetic Theory of Gases," McGraw-Hill, New York, N.Y., 1938, p. 291.

(19) S. Dushman, in "Scientific Foundations of Vacuum Technique," 2nd ed., J. M. Lafferty, Ed., Wiley, New York, N.Y., 1965, chap. 2.

(20) M. J. Zucrow and J. Hoffman, "Gas Dynamics," vol. I, Wiley, New York, N.Y., 1976, p. 12.

(21) T. K. Sherwood, R. L. Pigford, and C. R. Wilke, "Mass Transfer," McGraw-Hill, New York, N.Y., 1975, p. 39.

(22) *Ibid.*, p. 17.

(23) J. O. Hirshfelder, C. F. Curtis, and R. B. Bird, "Molecular Theory of Gases and Liquids," Wiley, New York, N.Y., 1954.

(24) R. B. Bird, W. E. Stewart, and E. N. Lightfoot, "Transport Phenomena," Wiley, New York, N.Y., 1960, p. 744.

(25) W. G. Pollard and R. D. Present, *Phys. Rev.*, **73**, 762 (1948).

(26) S. Dushman, in "Scientific Foundations of Vacuum Technique," 2nd ed., J. M. Lafferty, Ed., Wiley, New York, N.Y., 1965, p. 500.

(27) J. R. Dacey, in "Chemistry and Physics of Interfaces," D. E. Gushee, Ed., American Chemical Society, Washington, D.C., 1965, p. 151.

(28) E. R. Gilliland, R. F. Baddour, G. P. Perkinson, and K. J. Sladek, *Ind. Eng. Chem., Fundam.*, **13**, 95 (1974).

(29) K. J. Sladek, E. R. Gilliland, and R. E. Baddour, *ibid.*, **13**, 100 (1974).

NOTES

Flame-Ionization GLC Assay for Fluorouracil in Plasma of Cancer Patients

A. P. De LEENHEER ˣ and M. Cl. COSYNS-DUYCK

Received December 21, 1978, from the *Laboratoria voor Medische Biochemie en voor Klinische Analyse, Faculteit van de Farmaceutische Wetenschappen, Rijksuniversiteit, Academisch Ziekenhuis, 135 De Pintelaan, 9000-Gent, Belgium.* Accepted for publication February 20, 1979.

Abstract □ A rapid and specific flame-ionization GLC method was developed for the determination of plasma fluorouracil. The chloro analog is used as the internal standard. The method involves the isolation of both the drug and the internal standard from plasma on a strong anion-exchange column at pH 10. Elution is performed with acetic acid in methanol. The evaporated eluate is dissolved in tetrahexylammonium hydroxide. An aliquot of the resulting solution is introduced directly into the gas chromatograph, where conversion to the bishexyl derivatives and subsequent separation take place. The extraction recovery from blank plasma, to which fluorouracil was added, was 96.8 ± 2.4% (*SD*). Linearity was proven in the range from 0 to 25 μg/ml, whereas the detection limit of the method was estimated at about 2 μg/ml of plasma. The within-run precision was determined at three different fluorouracil levels. To demonstrate method applicability, plasma samples obtained from cancer patients to whom 1 g of fluorouracil had been administered intravenously were analyzed.

Keyphrases □ GLC, flame ionization—analysis, fluorouracil, human plasma, *in vivo* □ Antineoplastic agents—fluorouracil, flame-ionization GLC analysis, human plasma, *in vivo* □ Fluorouracil—analysis, flame-ionization GLC, human plasma, *in vivo*

Fluorouracil has been used for several years in the chemotherapeutic treatment of breast, stomach, and colon carcinoma. Different investigators administer fluorouracil in accordance with their own experience, using various dosage schedules (1–4). Systematic observation of fluorouracil disposition as a function of dosage schedule and route of administration in several patients would be valuable. Therefore, a rapid, sensitive, analytical method for fluorouracil determination in numerous biological samples is needed.

Besides the microbiological bioassays (5, 6), few chemical methods have been published. The spectrophotometric assay for fluorouracil (5) lacks specificity and sensitivity. GLC methods were reported using flame-ionization detection (7, 8), electron-capture detection (9), and multiple-ion detection (10–12). Most of these methods are based

0022-3549/79/0900-1174$01.00/0

© 1979, American Pharmaceutical Association